SPORT TK-EuroAmerican Journal of Sport Sciences

https://revistas.um.es/sportk Online ISSN: 2340-8812

Received: **09/02/2023.** Accepted: **25/04/2023.** Published: **17/04/2024**

Physical and psychological rehabilitation for common weightlifting injuries

Tang Xun Yang[1], Wei Wang[2]*, Elena Kozlova[3], Valentin Oleshko[1]

[1] Department of Combat Sports and Power Sport, National University of Ukraine on Physical Education and Sport, Kyiv, Ukraine.

[2] Department of Physical Education, Xihua University, Chengdu, China.

[3] Department of History and Theory of Olympic Sport, National University of Ukraine on Physical Education and Sport, Kyiv, Ukraine.

* Correspondence: Wei Wang; we.wang@wsdept.in.net

ABSTRACT

In the process of weightlifting, there is an increased load on both the respiratory system, the cardiovascular system, and on individual parts of the nervous system. At the same time, special attention is paid to the possibilities of providing a stable body functioning after the cancellation of treatment course and the corresponding pharmacological support of athletes with treatment schedule or without it. The novelty of the study is determined by the need to ensure constant and stable work of the cardiovascular system. The authors note that this is possible both when the body performance indicators return to the level before injury, and in conditions of returning to original sports results. It is determined in the paper that the use of the instrumental model will make it possible to develop sustainable energy consumption and coordinate the balancing of loads on an athlete during the period of recovery after injury. Model formation is based on uniform signals in a correlated random process in a simulation model. The practical significance of the study is determined by the need to structure the training loads in the post-traumatic period. This reduces a number of physiological and psychological stresses on a person and allows increasing in the long term the loads that the athlete plans to utilise after returning to the sports sector.

KEYWORDS

Stimulant; Formation; Model; Functioning

1. INTRODUCTION

According to the World Health Organisation (2020), coronary heart disease, which can occur after retirement from sports or during recovery from injury, is significantly more common than death from other sports-related injures (Wasik et al., 2015). Therefore, an important task of modern medicine is the diagnosis of coronary heart disease at the early stages of its onset and development (Sujadevi et al., 2017; Baimbetov et al., 2022). Devices for detecting coronary heart disease, common in medicine, use algorithms for processing an electrocardiosignal based on an analysis of its temporal structure (Gopika et al., 2019; Ahmad & Iqbal, 2022). In particular, the processing of the electrocardiosignal is performed on the ST-segment, since coronary heart disease is most strongly manifested in this segment, namely, in the form of a sharp increase or decrease in the amplitude, the occurrence of a break, or additional peaks (Yan et al., 2011; Nurtas et al., 2020). The process of disease manifestation, in which the structure of the cardiocomplex of the electrocardiosignal is examined and modelled, and the process of ischemic heart disease onset is shown. It consists in changing the angle of inclination of the ST-segment relative to the isoline, the possibility of changing the amplitude of this segment or the appearance of an additional break or peak at point "I" is determined by most specialists as primary (Kahankova et al., 2018). In the case of the use of described method of electrocardiosignal processing, information concentrated in other points of the segment is practically ignored (Cherif & Debbal, 2016).

The decision on the presence or absence of an ischemic episode is made based on observing the signal of the ST-segment of the current cardio complex or the signal averaged over a short time interval (Varshney & Singh, 2020). However, an ischemic episode develops within several seconds (Lehner & Rangayyan, 1987). Therefore, a significant part of the information not only about the presence of an ischemic episode but also about its course (if any) is practically lost during processing (Abadi & Sumarna, 2019). It is important to develop new, more effective processing methods for detecting coronary heart disease (El-Badlaoui & Hammouch, 2017). Common methods of electrocardiosignal processing to highlight informative characteristics that are indicators of coronary heart disease are associated with the study of the temporal structure and characteristics of the amplitude spectra of the electrocardiosignal (harmonic analysis methods) (Kouras et al., 2009). In the case of a probabilistic approach to modelling an electrocardiosignal, a stationary model is known, which determines the methods of spectral correlation analysis (Zhao et al., 2017). In this case, informative signs of a signal are its probabilistic characteristics and distributions (probabilities of values of a random variable, spectral power density, etc.) (Debbal & Bereksi-Reguig, 2008).

However, the stationary model does not have any means of describing oscillations in time, which are electrocardiosignals; therefore, the methods of spectral-correlation analysis do not make it possible to assess the phase-time characteristics of the signal in order to identify the moment of manifestation of changes in the structure of the electrocardiosignal, since such signal will be stationary only in the state of a medical norm and at short time intervals, because by its nature the electrocardiosignal is a nonstationarity type signal (Balasubramaniam & Nedumaran, 2010; Kluszczynski & Czernicki, 2012).

Often the possibility of diagnosing heart diseases is considered based on the findings from phonocardiographic signal processing, but for the purpose of identifying manifestations of coronary heart disease, this method provides limited opportunities, since the phonocardiographic signal itself reflects the work of the heart from the side of biomechanics, and information about the processes of excitation and relaxation of its individual departments in it are poorly expressed (Cherif et al., 2010; Baimbetov et al., 2018b). A model of the electrocardiosignal in the form of a periodically correlated random process has been substantiated, which will be adequate in the task of identifying manifestations of coronary heart disease (Kumar & Jagannath, 2015). Such model is a natural model of signals that have a rhythmic structure, and have the means of raising nonstationarity signals into stationary ones, without rejecting non-stationarity, but taking it into account, with the subsequent application of the methods of spectral-correlation analysis of the theory of stationary processes (Kim, 2015; Szczerba et al., 2021). The novelty of the study is determined by the need to ensure constant and stable work of the cardiovascular system.

2. METHODS

Based on empirical conclusions and actual medical facts, in particular, the fact that the problem of phonocardiographic signal transmission over the then existing analogue telephone lines with the appropriate parameters and bandwidth, the frequency response of which was "0.1 100 Hz", was successfully solved, using the "phonocardiographic signal bypass" obtained by passing the signal through analogue low-frequency filters, a simulation model of the phonocardiographic signal was developed in the form of an additive-multiplicative envelope of the mixture approximated by the sigmoid transition function and the vector of frequency content contracted from separate intervals previously shown in the frequency domain of white noise (Shino et al., 1996; Baimbetov et al., 2018a). Its main advantages include simplicity, undemanding machine resources, and the ability to take into account the randomness characteristic of the phonocardiographic signal (Had et al., 2020;

Kluszczynski et al., 2022). Based on the above and on the mathematical model of the phonocardiographic signal in the form of a periodically correlated random process; the computer simulation model has the form (1)-(2):

$$\xi(t)=\sum_{k}^{N_k}\left(\left\{\tilde{\xi}_k\left(\begin{array}{c}E\left(s_{nk},A_{nk}+\Psi_A,T_{nk},\nu_{nk},t_n\right)\\ \left(\begin{array}{c}wwn\left(T_{nk-oT_{n-1k}}\right)\\ 0\end{array}\right)\otimes h\left(f_{nkl}+\Psi_{f_{nkl}},f_{nkh}+\Psi_{f_{nkh}}\right)\end{array}\right)\right\}\begin{array}{l}t\in\left[T_{k-1},T_k\right)\\ t\notin\left[T_{k-1},t_k\right)\end{array}\right) \quad (1)$$

where $\tilde{\xi}_k$ – k-th contraction; N_k – number of phonocardiographic signal contractions; M_k – the number of intervals of the phonocardiographic signal within k-th contraction.

$$E(s_{nk},A_{nk},\Psi_A,T_{nk},\nu_{nk},t_n)=\begin{cases}\frac{A_{nk}}{1+\left(\frac{0,5T_{nk}}{t_n}\right)^{\nu_{nk}10}}+\Psi_A, s_{nk}>0\\ \frac{2A_{nk}}{1-\left(\frac{0,5T_{nk}}{t_n}\right)^{\nu_{nk}10}}+\Psi_A, s_{nk}<0\end{cases} \quad (2)$$

s_{nk} – marker of growth/decline of the approximating function of n-th interval of k-th contraction; A_{nk} – amplitude of n -th interval of k -th contraction; T_{nk} – duration of n-th interval of k -th contraction; ν_{nk} – growth / decline rate of n -th interval of k -th contraction; t_n – certainty interval of n-th interval; w – Blackman window; wn – white noise; o – overlap ratio of n -th interval with the dimension T_{nk} of k -th contraction relative to n-1-th interval T_{n-1k} of k -th contraction; $h\left(f_{nkl}+\Psi_{f_{nkl}},f_{nkh}+\Psi_{f_{nkh}}\right)$ – the kernel of convolution of the band pass filter from the lower f_{nl} and upper f_{nh} boundaries of the passband; $\Psi_{A_{nk}}\left(M(A_{nk}),D(A_{nk})\right),f_{nkl}\left(M(fi_{nkl}),D(fi_{nkl})\right),f_{nkh}\left(M(fi_{nkh}),D(fi_{nkh})\right)$ – random variables for amplitudes, low and high cut-off frequencies of the band-pass filter of n-th interval of k-th contraction with a Gaussian distribution law with mathematical expectation $M\{A\}=M(fi_{nkl})=M(fi_{nkh})=0$ sets of real numbers. According to this, a flowchart of the phonocardiographic signal simulation program was developed.

Thus, the hypothesis of the study is that weightlifting creates an increased load on the respiratory system, cardiovascular system and certain parts of the nervous system. Therefore, it is important to ensure the stable functioning of the body after the course of treatment and appropriate pharmacological support for athletes with or without a treatment schedule. Ensuring the constant and stable functioning of the cardiovascular system is possible by returning the body's performance indicators to the level that it was before the injury, or even better. An effective solution is to use an instrumental model to develop rational energy consumption and coordinate the balancing of loads on the athlete during the recovery period after an injury.

3. RESULTS AND DISCUSSION

The flowchart of the phonocardiographic signal simulation program (Figure 1) includes the following operations: at the stage of data initialisation, the program, after the start, makes settings for the environment and brings it to the default state, reads the values of the variables:

- T_{nk} – duration of n-th interval of k-th contraction;
- A_{nk} – amplitude of n-th interval of k-th contraction;
- s_{nk} – marker of growth/decline of the approximating function of n-th interval of k-th contraction; A_{nk} – amplitude of n -th interval of k -th contraction; T_{nk} – duration of n-th interval of k-th contraction; v_{nk} – rate of growth/decline of n -th interval of k -th contraction; t_n – interval of certainty of n-th interval; o – overlap ratio of n -th interval T_{nk} k-th contraction relative to $n-1$-th interval dimension T_{n-1k} of k-th contraction; f_{nl}– lower limit of the bandwidth; $f\_b\_ratio\_1$ – value of the first edge of the band pass filter; $f\_b\_ratio\_1$ – value of the second edge of the band pass filter; adjusts input parameters and makes initial settings of software objects and functions.

The next stage is the implementation of recursion by entering a global loop, the number of iterations of which depends on the number of heart contractions provided by the input data (variable k).

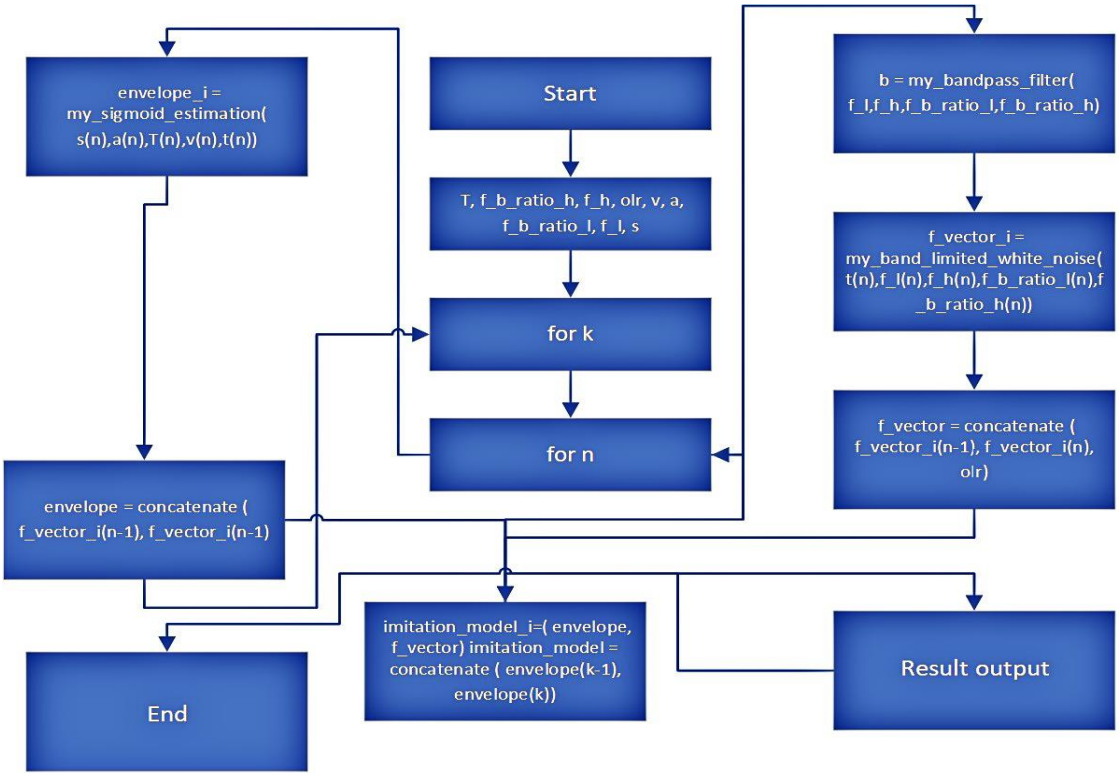

Figure 1. Sequence of operations for the implementation of the imitation model of the phonocardiographic signal

Then the recursion is occurred by entering a loop, the number of iterations of which depends on the number of n intervals of k-th contraction. Further, the algorithm is divided into two branches, which, provided there are more than one processor core in the system, can be performed in parallel and/or some of the computational operations can be implemented using the resources of the video adapter. The calculation of the transition function occurs at the next stage of the first branch of the algorithm of n -th interval of k -th contraction. Concatenation of the transition functions into the envelope vector occurs at the next stage of the first branch of the algorithm of n -th interval of k-th contraction. The synthesis of the bandpass filter (pole calculation) is the first stage of the second branch of the algorithm, which is responsible for the formation of the vector of frequency content. The generation of a fragment of bandpass white noise occurs at the next stage of the second branch of the algorithm of n-th interval of k-th contraction. Concatenation with overlapping fragments of bandpass white noise weighted with the Blackman window occurs at the next stage of the second branch of the algorithm of n-th interval of k-th contraction; Further, the ascent of both branches of the algorithm is reflected in one stream of calculating the resulting vector of the simulation model by forming a multiplicative mixture of the envelope and the frequency content vector. The algorithm performs each subsequent recursion of$k$ -th contraction to calculate the simulation model. The next stage is to save the calculation results and display the results in a graphical form convenient for analysis by the user.

The final step is to clean up the workspace, reset the environment to its default state, check the checksums, and exit the runtime. Software development is carried out in the Matlab environment, which combines many high-level abstraction tools and allows simplifying this stage, and thereby reduce the cost of the final product. A subroutine for extracting the envelope of a real phonocardiographic signal. The flowchart of the program is shown in the Figure 2.

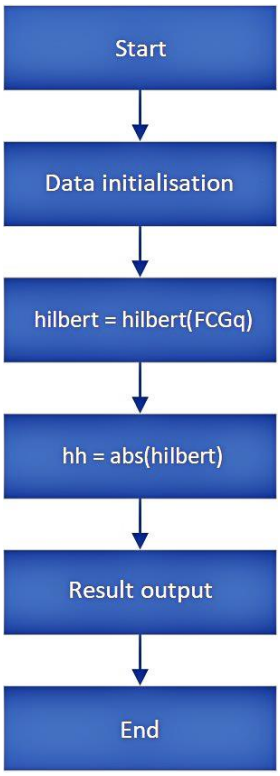

Figure 2. The flowchart for extracting the envelope of an actual signal

The flowchart of the subroutine for extracting the envelope of an actual signal includes the following operations: at the stage of data initialisation, the program, after starting, makes settings for the environment and reads the values of the variables to the default state; the next step is the calculation of the Hilbert transform and, accordingly, the selection of the orthogonal conjugation; then the bypass phonocardiogram is calculated by the expression (3):

$$envelope = \sqrt{x_r^2 + x_i^2} \tag{3}$$

To speed up the algorithm, it was decided to synthesise a Hilbert phase splitter with the following characteristic: the next stage is to save the calculation results and output of the results, clean up the workspace, bring the environment to the default state, check checksums and exit the program code execution environment. The impulse response of the Hilbert phase inverter is calculated by the expression (4):

$$H\left(e^{j\omega}\right) = \sum_{-\infty}^{\infty} h[n] e^{-j\omega} \tag{4}$$

As a result of the filtering procedure of the Hilberat phase splitter, two sequences were obtained – the real and imaginary parts of the complex vector (5):

$$x_i[m] = \sum_{-\infty}^{\infty} h[n-m]\, x_r[m], \tag{5}$$

$$x_r[m] = \sum_{-\infty}^{\infty} h[n-m]\, x_i[m]$$

And the alternative phonocardiographic signal is calculated by the expression, which is the final (6):

$$envelope = \sqrt{x_r^2 + x_i^2} \tag{6}$$

Flowchart of the subroutine for generating the conjugation function for approximation of the phonocardiographic signal bypass: at the stage of data initialisation, the program, after starting, makes settings for the environment and reads the values of the variables to the default state; the next step is a block of conditions that depend on s_{nk} (the marker of growth/decline of the sigmoid function is "true" at $s_{nk} > 0$ and "insignificant" at $s_{nk} < 0$; then the generation of the conjugation function for the approximation is calculated by the formula (7):

$$g = a./\left(1 + (0{,}5 * T./(t_n + eps)\right).\hat{}\,(v * 10)) \tag{7}$$

when $s_{nk} > 0$
or (8):

$$g = a + a./-\left(1 + (0{,}5 * T./(t\_n + eps)\right).\hat{}\,(v^*)) \tag{8}$$

when $s_{nk} < 0$;

The next stage – saving the calculation results and outputting the results, clearing the workspace, bringing the environment to its default state, checking the checksums and exiting the program code execution environment. Generation of the conjugation function for an approximation of the phonocardiographic signal alternative is calculated by the expression (9):

$$E(s_{nk}, A_{nk}, \Psi_A, T_{nk}, \nu_{nk}, t_n) = \begin{cases} \frac{A_{nk}}{1+\left(\frac{0{,}5T_{nk}}{t_n}\right)^{\nu_{nk}10}} + \Psi_A, s_{nk} > 0 \\ \frac{2A_{nk}}{1-\left(\frac{0{,}5T_{nk}}{t_n}\right)^{\nu_{nk}10}} + \Psi_A, s_{nk} < 0 \end{cases} \tag{9}$$

N_k – number of phonocardiographic signal contractions; M_k – number of phonocardiographic signal intervals within$k$ -th contraction; s_{nk} – marker of growth/decline of the approximating function of n -th interval of k -th contraction; A_{nk} – amplitude of n -th interval of k -th contraction; T_{nk} – duration of n -th interval of k -th contraction; ν_{nk} – rate of growth/decline of n -th interval of k -th contraction; t_n – certainty interval of n -th interval; w – Blackman window.

Based on the above mathematical apparatus, a flowchart of the subroutine for generating the structure of a bandpass filter (Figure 3) has been drawn up, including the following operations: at the stage of data initialisation, the program, after starting, sets up the environment and brings it to its default state. Carries out setting of input parameters and carries out initial settings of software objects and functions; syntheses the desired filter (poles b) given the values of the variables: t_n – certainty interval of n-th interval; o – overlap ratio of n-th interval with dimensionality T_{nk} of k -th contraction relative to n−1-th interval with dimensionality T_{n-1k} of k-th contraction; f_{nl} – bandwidth lower limit; f_{nh} – bandwidth upper limit; $f\_b\_ratio\_1$ – value of the first edge of the band pass filter (0.15); $f\_b\_ratio\_h$ – the value of the second edge of the band pass filter (0.15); the next stage is saving the results of the calculation and displaying the results, clearing the workspace, bringing the environment to its default state, checking the checksums and exiting the runtime.

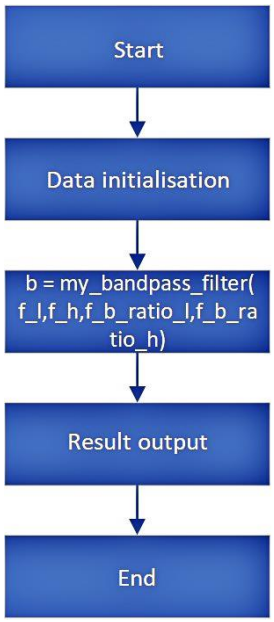

Figure 3. The flowchart of bandpass filter structure generation

The structure of the bandpass filter is generated according to the expression (10):

$$h(n) = f\left(x, f_{nkl} + \Psi_{f_{nkl}}, f_{nkh} + \Psi_{f_{nkh}}\right) \quad (10)$$

where $f_{nkl}\left(M(fi_{nkl}), D(fi_{nkl})\right)$ and $f_{nkh}\left(M(fi_{nkh}), D(fi_{nkh})\right)$ – random variables for amplitudes, low and high cutoff of bandpass filter of n -th interval of k -th contraction with Gaussian distribution with mathematical expectation $M\{A\} = M(fi_{nkl}) = M(fi_{nkh}) = 0$ and variances $D(fi_{nkl}), D(fi_{nkh})$. $k \in Z, n \in Z$ – sets of real numbers.

A flowchart of band-limited noise generation is shown in the Figure 4.

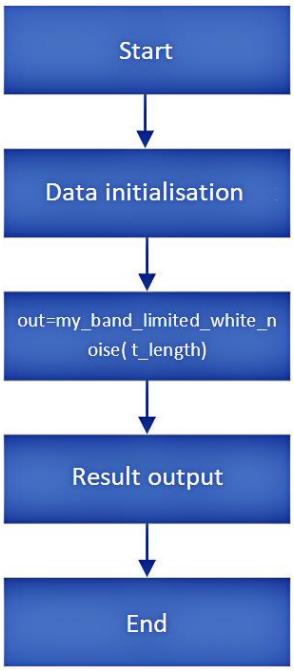

Figure 4. The flowchart of band-limited noise generation

Flowchart of the subroutine for generating band-limited noise: at the stage of data initialisation, the program, after starting, makes settings for the environment and brings it to the default state and reads the values of the variables; further, band-limited noise is generated depending on the same variables as for the subroutine for generating the band-pass filter structure; the next stage is saving the results of the calculation and displaying the results, clearing the workspace, bringing the environment to its default state, checking the checksums and exiting the program code execution environment. The distribution density of the signal has the shape of a Gaussian curve, which corresponds to a normal distribution. Band-limited noise is generated according to the expression:

$$wn_{bl} = \left(w\, wn\left(T_{nk-o\,T_{n-1k}}\right)h(f_{nkl} + \Psi_{f_{nkh}}, f_{nkh} + \Psi_{f_{nkh}}\right) \quad (11)$$

where w – Blackman window; wn – white noise; $h\left(f_{nkl} + \Psi_{f_{nkl}}, f_{nkh} + \Psi_{f_{nkh}}\right)$ – bandpass filter convolution kernel.

As a result of processing phonocardiographic signal and a dedicated bypass signal, it performs approximation of the bypass signal using a sigmoid function. In this case, the corresponding vector of the unit amplitude of the phonocardiographic signal frequency filling is generated in accordance with physiological data. One of the most common and at the same time the most informative methods for studying stationary signals is the windowed Fourier transform. This approach makes it possible to see the instantaneous amplitude of each harmonic over time. The classical Fourier transform takes into account the spectrum of the signal, which is taken over the entire range of existence of the variable.

Most often, interests are focused only on the local distribution of frequencies, while it is necessary to preserve the primary variable (usually time). In this case, a generalised Fourier transform is used, the so-called windowed Fourier transform. First, we need to select some window function (12):

$$F(t,\omega)=\frac{1}{\sqrt{2\pi}}\sum_{-\infty}^{\infty}f(\tau)W(\tau-t)e^{-i\omega\tau}d\tau \quad (12)$$

where $F(t,\omega)$ – gives the frequency distribution of a part of the original signal $f(t)$ over time t; $W(\tau-t)$ – sliding window function.

Let the images $f(n1,n2)$ and $g(n1,n2)$ be described by models of homogeneous random fields. The degree of correspondence of a real image to an ideal one can be the mean value of the square of their difference (13):

$$\varepsilon_{kv}^2 = E\{(f-g)^2\} \quad (13)$$

This value will be constant throughout the entire field of arguments, therefore, the arguments (the same for *f*, *g*) are omitted for brevity. If the mathematical expectations f and g are equal, then the difference has a zero mean, and the value ε_{kv}^2 takes on the meaning of the variance of the difference (and the value of the standard deviation of g from *f*) of two images. For a stationary model, it is usually assumed that the ergodicity condition is satisfied, under which averaging over an ensemble of contractions can be replaced by averaging over one contraction. Then for continuous images at (14):

$$0 \le n_1 \le N_1-1,\ 0 \le n_2 \le N_2-1 \quad (14)$$

we obtain (15):

$$\varepsilon_{kv}^2 \approx \frac{1}{4L_1L_2}\int_{-L_1}^{L_2}\int_{-L_1}^{L_2}\left[f(x_1,x_2)-g(x_1,x_2)\right]^2 dx_1dx_2 \quad (15)$$

and for discrete data we obtain (16):

$$\varepsilon_{kv}^2 \approx \frac{1}{4N_1N_2}\sum_{n_1=0}^{N_1-1}\int_{n_{21}=0_1}^{N_{21}-1}\left[f(n_1,n_2)-g(n_1,n_2)\right]^2 \quad (16)$$

The result of calculating the root-mean-square criterion is 0.035; which is close to an unbiased estimate of the standard deviation of the normal distribution of one sample. Dispersion (17):

$$D[x]=\sigma^2;\ \sigma^2=\frac{\sum(x_i-a)^2n_i}{\sum n_i};\ \sigma=\sqrt{D}=\sqrt{0{,}001225}=0{,}035) \quad (17)$$

Therefore, an objective assessment indicates the correspondence of the simulation model to the real signal. Assessment of the reliability of a selected mathematical model of the phonocardiographic signal is simultaneously registered as a periodically correlated random process; carried out in the time domain using first-order statistics, namely: 50 values of the arithmetic mean of

the stationary components of the phonocardiographic signal (variance over contractions) were calculated at 50 intervals, each of which was 10 contractions of the phonocardiographic signal cut out along the P-waves with a duration of 10 contractions, provided that in at each interval, the heart rate variation is less than 5% (Baimbetov et al., 2020). In addition to calculating the kurtosis and asymmetry coefficients, the distribution normality of the sequence under study was estimated using the Kolmogorov-Smirnov consistency criterion, which is used to test hypotheses regarding continuous distribution laws of quantities. The Kolmogorov-Smirnov criterion allows checking the consistency of the empirical distribution function with the theoretical one. The validity of the hypothesis is tested (18):

$$H_{0:}F^*(x) = F(x) \tag{18}$$

contrary to hypothesis (19):

$$H_{1:}F^*(x) \neq F(x) \tag{19}$$

Kolmogorov's goodness-of-fit test is based on the fact that the distribution of the difference between the theoretical and empirical distribution functions (20):

$$D_n = sup|F^*(x) - F(x)| \tag{20}$$

Is the same for every $F(x)$. The value D_n is called the Kolmogorov statistics.

For small n tables of critical points D_{kr} exist for the Kolmogorov statistics. For big n the limit Kolmogorov distribution is used (21):

$$P\left(\sqrt{n}D_n < x\right) \to Q\left(x\right) = 1 + 2\sum_{k=1}^{\infty}\left(-1\right)^{k-1} e^{-2k^2x^2}, n \to \infty \tag{21}$$

For the Kolmogorov distribution, the limit for the statistics of cell $\lambda = \sqrt{n}D_n$ there are also tables of critical points λ_{kr}. In practice, they are used at $n > 20$. The statistic $\lambda = \sqrt{n}D_n$ do not depend on the type of the unknown distribution function. In the general case, the distribution function $F(x)$ can be discontinuous, although they should be discontinuities of the first kind, abrupt changes. Therefore, sample statistic λ are generally determined using the exact upper bound (sup) (22)–(23):

Smirnov statistic (22):

$$D_n^- = \sup_x [F(x) - F^*(x)], \lambda = \sqrt{n}D_n^- \tag{22}$$

Kolmogorov statistic (23):

$$D_n^+ = \sup_x [F^*(x) - F(x)], \lambda = \sqrt{n}D_n^+ \tag{23}$$

in addition (24):

$$D_n = \max_x [D_n^-, D_n^+] \tag{24}$$

In this case, the hypothesis testing algorithm looks like this:

1) the input data are presented as an interval statistical (variation) series;

2) the value of the empirical distribution function $F^*(x)$ is found;

3) using a hypothetical distribution function, the value $F^*(x)$ of the theoretical distribution function is considered, which corresponds to the input data of the random variable ξ;

4) D_n is found and the observed value of the sample statistic $\lambda_H = \sqrt{n}D_n$ is calculated.

5) for a given level of significance α critical points λ_α are found from the tables of quantiles of the Kolmogorov distribution;

6) comparing the observed values of the sample statistics λ_H with the critical point λ_α one of two decisions is made: if $D_n\sqrt{n} < \lambda_\alpha$, then, it is considered that there are no reasons for rejecting the null hypothesis, that is, the hypothetical distribution function is consistent with the investigated data on the phonocardial signal dispersion at 50 intervals; if $D_n\sqrt{n} > \lambda_\alpha$, then the null hypothesis is rejected in favour of an alternative.

It is important that the Kolmogorov criterion cannot be applied in the case of grouped data. The algorithm for calculating the Kolmogorov-Smirnov consistency criterion is also implemented in the syntax of the Matlab programming language. The calculated value of the Kolmogorov-Smirnov test is 0.0075 with a critical value of 0.009, which allows us to accept the null hypothesis and assert that the distribution of variances of stationary components over 50 intervals is normal, and the p-value of the test is equal to 0.2017 (a scalar value in the range [0, 1]) is interpreted as the probability of observing the test statistic as extreme, or more extreme than the value observed under the null hypothesis. Small p values call into question the validity of the null hypothesis. An important approach to developing a rule for choosing solutions in the absence of a priori information about losses and the probability of states is the Neumann-Pearson criterion. In accordance with this criterion, a rule is chosen that provides the minimum possible value β of the second kind probability, provided that the probability of an error of the first kind does not exceed a given value α. Among all the criteria that distinguish between hypotheses H_0, H_1 with a given first kind error α, the most significant is the likelihood ratio criterion. According to the Neumann-Pearson theorem, there is a constant C, depending only on α, while the critical region S of the most significant criterion has the form (25):

$$S = \left\{x: W_n(x_1, \dots, x_n|s_0) \cup \frac{W_n(x_1,\dots,x_n|s_1)}{W_n(x_1,\dots,x_n|)s_0} > C, W_n(x_1, \dots, x_n|s_0) \neq 0\right\} \quad (25)$$

Where the constant C is a solution to the equation (26):

$$P\left(\frac{W_n(x_1,\ldots,x_n|s_1)}{W_n(x_1,\ldots,x_n|s_0)} > C|s_0\right) = \alpha \quad (26)$$

The rule for choosing a solution according to the Neumann-Pearson criterion has the greatest significance among all other rules for which the significance level does not exceed α. As a consequence, it is possible to maximise the value (27):

$$1-\beta = \int_S = W_n\left(x_1,\ldots,x_n \mid s_1\right) dt_1 \ldots dt_n \quad (27)$$

provided (28) that:

$$\int_S W_n\left(x_1,\ldots,x_n \mid s_1\right) dt_1 \ldots dt_n = \alpha \quad (28)$$

The set $T = \{x: W_n(x_1, \ldots, x_n|s_0) = 0\}$ does not change the value of the criterion α, but increases its significance. It is accepted that $T \subseteq S$, for the case $S \subseteq R_n \backslash T$. Therefore (29):

$$1-\beta = \int_S \frac{W_n\left(x_1,\ldots,x_n \mid s_1\right)}{W_n\left(x_1,\ldots,x_n \mid s_0\right)} W_n\left(x_1,\ldots,x_n \mid s_0\right) dt_1 \ldots dt_n \quad (29)$$

given that (30):

$$\int_S W_n\left(x_1,\ldots,x_n \mid s_1\right) dt_1 \ldots dt_n = \alpha \quad (30)$$

As a consequence, the mean value of the random variable is maximised (31):

$$l(x_1,\ldots,x_n) = \frac{W_n(x_1,\ldots,x_n|s_1)}{W_n(x_1,\ldots,x_n|s_0)} \quad (31)$$

provided that the null hypothesis H_0 is true. The decision selection rule based on the Neumann-Pearson criterion is a special case of the Bayesian solution in which the quantity $\frac{q}{p}C$ is replaced by the quantity C. Since if the null hypothesis H_0 is true, the random variable (32):

$$\bar{x} \in N\left(a_0, \frac{\sigma^2}{n}\right), \frac{(\bar{x}-a_0)}{\sigma}\sqrt{n} \in N(0,1) \quad (32)$$

then the probability of getting into the critical region is (33):

$$P(S\backslash H_0) = P(\bar{x} \geq C_1, a = a_0) = 1 - F\left[\frac{(C_1-a_0)\sqrt{n}}{\sigma}\right] = \frac{1}{2} - \Phi\left[\frac{(C_1-a_0)\sqrt{n}}{\sigma}\right] = \alpha \quad (33)$$

where $\Phi\left(x\right) = \frac{1}{\sqrt{2\pi}}\int_0^x e^{-\frac{t^2}{2}} dt$ – normal distribution function related to the integral Laplace function by the relation (34):

$$F(x) = \Phi(x) + \frac{1}{2} \quad (34)$$

Let us denote u_a as the solution of the equation (35):

$$\Phi(x) = \frac{1}{2} - \alpha \quad (35)$$

Quantity u_α with level quantile (36):

$$\frac{1-2\alpha}{2} \tag{36}$$

for the standard normal distribution and is taken as the critical point. Its values are found from the table of the Laplace function with the condition (37):

$$\Phi\left(u_\alpha\right)=\frac{1}{2}-\alpha \tag{37}$$

Then from the equation (38):

$$\Phi\left[\frac{\left(C_1-a_0\right)\sqrt{n}}{\sigma}\right]=\frac{1}{2}-\alpha \tag{38}$$

from the tables of the Laplace function, the quantile u_α is found and the constant C_1 is determined assuming that (39):

$$\frac{(C_1-a_0)\sqrt{n}}{\sigma}=u_\alpha \tag{39}$$

or (40):

$$C_1=a_0+\frac{\sigma}{\sqrt{n}}u_\alpha \tag{40}$$

The criterion for testing a hypothesis is formulated as follows: if $a_0 < C_1 < a_1$, then at $\bar{x} > C_1$ the hypothesis H_1 is accepted, and at $\bar{x} \le C_1$ the hypothesis H_0 is accepted.

Thus, the most significant criterion for testing a hypothesis H_0: $a = a_0$ with an alternative H_1: $a = a_1$:
whereas (41):

$$\bar{x} \ge a_0+\frac{\sigma}{\sqrt{n}}u_\alpha \tag{41}$$

then hypothesis H_0 is rejected,
whereas (42):

$$\bar{x} < a_0+\frac{\sigma}{\sqrt{n}}u_\alpha \tag{42}$$

then hypothesis H_0 is accepted.

If the hypothesis H_0 is correct, but an event $\bar{x} > C_1$ has occurred, then the hypothesis H_1 is accepted, that is, an error of the first kind. If the hypothesis H_1 is correct, but an event $\bar{x} \le C_1$ has occurred, then the hypothesis H_0 is accepted, then this is an error of the second kind. An important negative factor, the influence of which must be minimised, is the breathing. To assess the reliability of the processing results, the CFAR method (Constant False Alarm Rate or the constant probability of false alarms) was used, which is a modification of the Neumann-Pearson statistical criterion and is

adaptive, which makes it possible to assess the reliability of the phonocardial signal processing results. The reliability of estimates is calculated by the formula (43):

$$P_d = \frac{sum(D>T)}{N_{trial}} \quad (43)$$

where P_d – reliability value, which in terms of Monte Carlo modeling is the ratio of the number of sections to the "number of attempts", that is, the total length of the sequence under consideration; D – averaged values of the variance of the phonocardiographic signal samples;

dynamic discrimination threshold calculated in a sliding window (44):

$$T = aP_n \quad (44)$$

scale factor (45):

$$a = N\left(P_{fa}^{-1/N} - 1\right) \quad (45)$$

average of readings x_m of the worked out sequence in a window of length N (46):

$$P_n = \frac{1}{N}\sum_{m=1}^{N} x_m \quad (46)$$

false alarm probability; erf – error function (47):

$$P_{fa} = \frac{1}{2}\left[1 - erf\left(\sqrt{SNR}\right)\right] \quad (47)$$

square root of the signal-to-noise ratio; N_s – signal significance; M_s – gain of the matched filter; T_{mf} – threshold after matched filter (48):

$$\sqrt{SNR} = \frac{T_{mf}}{\sqrt{N_s M_s}} \quad (48)$$

4. CONCLUSIONS

Results of the calculated instantaneous confidence values P_d of the reliability of the stationary components of the phonocardiographic signal at the given probabilities of error $P_{fa} = (0{,}001;\ 0{,}01;\ 0{,}1)$, indicate that the estimates of the stationary components of the phonocardiographic signal are invariant-informative signs that can be used to assess the state of the cardiovascular system with high reliability (0.9784-0.9872) in a person (in a normal state or with medical condition) at an early stage of the development of pathology, which confirms the adequacy of the mathematical model of the phonocardiographic signal simultaneously recorded in the form of a periodically correlated random process. To minimise the possibility of an error of the second kind and, given the fact that the signal under study is stochastic, a double verification of the simulation results by introducing an additional procedure for assessing the results obtained using the Smirnov

homogeneity criterion, which is used to test the hypothesis that two independent samples belong to the same th distribution law. It was found that the reliability of the results is (0.9873-0.9952). The authors have created a test signal with known parameters, made changes to it, and processed the test signal by the proposed method for experimental verification of the theoretical results of phonocardiographic signal processing. It was found that the method is suitable for processing phonocardiographic signals.

5. REFERENCES

Abadi, A. M., & Sumarna. (2019). Construction of fuzzy system for classification of heart disease based on phonocardiogram signal, 64-69. In: *Proceedings – 2019 1st International Conference on Artificial Intelligence and Data Sciences*. Ipoh: Institute of Electrical and Electronics Engineers (IEEE).

Ahmad, S., & Iqbal, T. (2022). The role of management commitment in adoption of occupational health and safety at higher education institutions. *Entrepreneurship and Sustainability Issues*, *9*(3), 103-117. http://doi.org/10.9770/jesi.2022.9.3(7)

Baimbetov, A., Bizhanov, K., Yakupova, I., Bairamov, B., Medeubekov, U., & Madyarov, V. (2020). Long-term results of simultaneous hybrid ablation of therapy-resistant atrial fibrillation. *European Heart Journal*, *41*, 626-626.

Baimbetov, A., Bizhanov, K., Yergeshov, K., Bayramov, B., Yakupova, I., & Bozshagulov, T. (2018a). One year continuously monitoring follow up results after single procedure atrial fibrillation ablation using cryoballoon second generation. *European Heart Journal*, *39*, 1225-1225.

Baimbetov, A., Kuzhukeyev, M., Bizhanov, K., Ergeshov, K., Yakupova, I., Bozshagulov, T., & Ismailova, G. (2018b). Atrial fibrillation ablation using second-generation cryoballoon. Cryoballoon ablation. *New Armenian Medical Journal*, *12*(1), 64-71.

Baimbetov, A.K., Abzaliev, K.B., Jukenova, A.M., Bizhanov, K.A., Bairamov, B.A., & Ualiyeva, A.Y. (2022). The efficacy and safety of cryoballoon catheter ablation in patients with paroxysmal atrial fibrillation. *Irish Journal of Medical Science*, *191*(1), 187-193. https://doi.org/10.1007/s11845-021-02560-z

Balasubramaniam, D., & Nedumaran, D. (2010). Design and development of digital signal processor based phonocardiogram system, 366–370. In: *International Conference on Signal Acquisition and Processing*. Bangalore: Institute of Electrical and Electronics Engineers (IEEE).

Kumar, S., & Jagannath, M. (2015). Analysis of Phonocardiogram signal for biometric identification system, pp. 233-243. In: *International Conference on Pervasive Computing: Advance Communication Technology and Application for Society*. Pune: Institute of Electrical and Electronics Engineers (IEEE).

Cherif, L. H., & Debbal, S. M. (2016). Optimal nodes combination of a wavelet packet tree for phonocardiogram signal analysis. *International Journal of Innovative Computing*, *12*(1), 215-224.

Cherif, L. H., Debbal, S. M., & Bereksi-Reguig, F. (2010). Choice of the wavelet analyzing in the phonocardiogram signal analysis using the discrete and the packet wavelet transform. *Expert Systems with Applications*, *37*(2), 913-918. https://doi.org/10.1016/j.eswa.2009.09.036

Debbal, S. M., & Bereksi-Reguig, F. (2008). Filtering and classification of phonocardiogram signals using wavelet transform. *Journal of Medical Engineering and Technology*, *32*(1), 53-65. https://doi.org/10.1080/03091900600750348

El Badlaoui, O., & Hammouch, A. (2017). Phonocardiogram classification based on MFCC extraction, 217–221. In: *International Conference on Computational Intelligence and Virtual Environments for Measurement Systems and Applications*. Annecy: IEEE.

Gopika, P., Sowmya, V., Gopalakrishnan, E. A., & Soman, K. P. (2019). Performance improvement of deep learning architectures for phonocardiogram signal classification using fast fourier transform, pp. 290–294. In: *Proceedings of the 2019 9th International Conference on Advances in Computing and Communication*. Kochi: IEEE.

Had, A., Sabri, K., & Aoutoul, M. (2020). Detection of Heart Valves Closure Instants in Phonocardiogram Signals. *Wireless Personal Communications*, *112*(3), 1569-1585. https://doi.org/10.1007/s11277-020-07116-5

Kahankova, R., Martinek, R., Jaros, R., Nedoma, J., Fajkus, M., & Vanus, J. (2018). Least Mean Squares Adaptive Algorithms Optimization for Fetal Phonocardiogram Extraction. *IFAC-PapersOnLine*, *51*(6), 60-65. https://doi.org/10.1016/j.ifacol.2018.07.130

Kim, D. J. (2015). Formant detection technique for the phonocardiogram spectra using the 1st and 2nd derivatives. *Transactions of the Korean Institute of Electrical Engineers*, *64*(11), 1605-1610. https://doi.org/10.5370/KIEE.2015.64.11.1605

Kluszczynski, M., & Czernicki, J. (2012). Analysis of Changes in Selected Body Characteristics in Many Years of Observation of Children and Adolescents with Faulty Body Posture. *Studies in Health Technology and Informatics*, *176*, 465-465.

Kluszczynski, M., Pilis, A., & Czaprowski, D. (2022). The importance of the size of the trunk inclination angle in the early detection of scoliosis in children. *BMC Musculoskeletal Disorders*, *23*(1), 5. https://doi.org/10.1186/s12891-021-04965-4

Kouras, N., Boutana, D., Benidir, M., & Barkat, B. (2009). A comparative study of some wavelet functions in the denoising of phonocardiogram signals, pp. 25-32. In: *Proceedings of the 2nd International Conference on Advanced Computer Theory and Engineering.* Cairo: Amer Society of Mechanical. 323 p.

Lehner, R. J., & Rangayyan, R. M. (1987). A Three–Channel Microcomputer System for Segmentation and Characterization of the Phonocardiogram. *Browse Journals & Magazines*, *34*(6), 485-489.

Nurtas, M., Baishemirov, Z., Tsay, V., Tastanov, M., & Zhanabekov, Z. (2020). Applying neural network for predicting cardiovascular disease risk. *News of the National Academy of Sciences of the Republic of Kazakhstan-Series Physico-Mathematical*, *4*(332), 28-34. https://doi.org/10.32014/2020.2518-1726.62

Shino, H., Yoshida, H., Yana, K., Harada, K., Sudoh, J., & Harasawa, E. (1996). Detection and classification of systolic murmur for phonocardiogram screening, pp. 123-124. In: *Annual International Conference of the IEEE Engineering in Medicine and Biology – Proceedings*. Amsterdam: IEEE. 2340 p.

Sujadevi, V. G., Soman, K. P., Sachin Kumar, S., Mohan, N., & Arunjith, A. S. (2017). Denoising of phonocardiogram signals using variational mode decomposition, pp. 1443-1446. In: *International Conference on Advances in Computing, Communications and Informatics.* Udupi: IEEE. 2409 p.

Szczerba, E., Kaminska, K., Mierzwa, T., Misiek, M., Kowalewski, J., & Lewandowska, M.A. (2021). BRCA1/2 Mutation Detection in the Tumor Tissue from Selected Polish Patients with

Breast Cancer Using Next Generation Sequencing. *Genes*, *12*(4), 519. https://doi.org/10.3390/genes12040519

Varshney, S., & Singh, S. (2020). Computation of biological murmurs in phonocardiogram signals using fast fourier discrete wavelet transform, pp. 234-240. In: *Proceedings of International Conference on Computation, Automation and Knowledge Management*. Dubai: IEEE. 559 p.

Wasik, J., Motow-Czyz, M., Shan, G. B., & Kluszczynski, M. (2015). Comparative analysis of body posture in child and adolescent taekwon-do practitioners and non-practitioners. *Ido Movement for Culture-Journal of Martial Arts Anthropology*, *15*(3), 35-40. https://doi.org/10.14589/ido.15.3.5

Yan, H., Wei, X., Han, F., & Lin, J. (2011). Monitoring the impact of general anesthesia induction and endotracheal intubations on cardiac performance by phonocardiogram. *Biomedical Engineering – Applications, Basis and Communications*, *23*(3), 231-236. https://doi.org/10.4015/S1016237211002566

Zhao, Z., Zhang, X., Fang, Z., Chen, X., Du, L., & Li, T. (2017). Phonocardiogram Segmentation and Abnormal Phonocardiogram Screening Algorithm Based on Cardiac Cycle Estimation. Dianzi Yu Xinxi Xuebao. *Journal of Electronics and Information Technology*, *39*(11), 2677-2683. https://doi.org/10.11999/JEIT170108

AUTHOR CONTRIBUTIONS

All authors listed have made a substantial, direct and intellectual contribution to the work, and approved it for publication.

CONFLICTS OF INTEREST

The authors declare no conflict of interest.

FUNDING

This research received no external funding.

COPYRIGHT